

Exotic magnetism and superconductivity in Ge-substituted CeCu₂Si₂: A Cu NQR studyY. Kawasaki,* K. Ishida,[†] K. Obinata, K. Tabuchi, K. Kashima, and Y. Kitaoka*Department of Physical Science, Graduate School of Engineering Science, Osaka University, Toyonaka, Osaka 560-8531, Japan*

O. Trovarelli, C. Geibel, and F. Steglich

Max-Planck Institute for Chemical Physics of Solids, D-01187 Dresden, Germany

(Received 4 October 2001; revised manuscript received 28 May 2002; published 6 December 2002)

We report Cu NQR results on Ge-doped heavy-fermion superconductors CeCu₂(Si_{1-x}Ge_x)₂ ($0 < x \leq 0.2$) and compare with previous results on Ce_{0.99}Cu_{2.02}Si₂ ($x=0$). Once only 1% Ge is substituted for Si to expand the lattice, an antiferromagnetic (AFM) order sets in at $T_N \sim 0.7$ K, followed by the onset of superconductivity at $T_c = 0.5$ K. The sudden emergence of AFM order due to the slight Ge doping reinforces that an exotic magnetic phase at $x=0$ is in fact a marginal AFM state where slowly fluctuating AFM waves propagate over a long distance. The appearance of internal fields throughout the sample that is deduced from the NQR spectral shape below T_N , excludes the presence of phase segregation between the superconducting (SC) and the AFM phases in the coexistent state below T_c . The $1/T_1$ result does not show significant reduction below T_c , followed by a $T_1 T = \text{const}$ behavior. This indicates that the SC phase is in a gapless regime, dominated by magnetic excitations due to the coexistence of AFM and SC phase. As Ge content increases, T_N is progressively increased, while T_c is steeply decreased. As a result of the suppression of the slowly fluctuating AFM waves in the samples with more than $x=0.06$, their magnetic properties above T_N progressively change to those in a localized regime as observed in CeCu₂Ge₂. The exotic interplay between magnetism and superconductivity in $0 \leq x < 0.06$ is discussed in the context of a SO(5) theory that unifies superconductivity and antiferromagnetism.

DOI: 10.1103/PhysRevB.66.224502

PACS number(s): 74.70.Tx, 71.27.+a, 74.62.Dh, 76.60.-k

I. INTRODUCTION

Heavy-fermion (HF) superconductivity has received much attention with respect to the intimate relation between magnetism and superconductivity. Up to now, it has been established that the superconductivity in Ce-based HF compound appears close to a magnetic phase. Actually, a number of HF compounds are shown to exhibit superconductivity around a critical pressure where some kind of magnetic order is suppressed by applying pressure (P).¹⁻⁴ In contrast, the superconductivity in underlying compound CeCu₂Si₂ emerges just at the border of the antiferromagnetic (AFM) phase at ambient pressure ($P=0$). This was demonstrated by the existence of a magnetic phase adjacent to the superconducting (SC) state. When magnetic field (H) exceeds its upper critical field, the field induced normal state is replaced by magnetic phase A .⁵ Although the nature of phase A is still unknown, it was shown to be magnetic in origin by several experiments.⁵⁻⁷

From the Cu-NQR measurements,⁸ we suggested that phase A at $H=0$ behaves as a marginal AFM state, where slowly fluctuating AFM waves propagate over a long distance and coexist with the SC state. It is quite unusual that their characteristic frequency ($\omega_c \sim 3 \times 10^6 \text{ sec}^{-1}$) is extremely low and comparable to a Cu-NQR frequency in this compound.⁹ Therefore, this marginal AFM state that sets in well above T_c , wipes out the NQR intensity.⁶ This wipe-out effect was reported in high- T_c cuprates La_{2-x}Sr_xCuO₄ as well.^{10,11} Thereby, the emergence of slowly fluctuating AFM waves seems to be one of characteristics for strongly correlated electron systems nearby the AFM phase.

These exotic magnetic and SC properties in

Ce_{0.99}Cu_{2.02}Si₂ ($T_c \sim 0.65$ K) have been extensively investigated through the transport, thermal, and NQR measurements.^{9,12-24} From these studies, it was clarified that Ce_{0.99}Cu_{2.02}Si₂ is just at the border to the AFM phase and that exotic superconductivity manifests itself under the unconventional normal state where the slowly fluctuating AFM waves propagate over a long range without any trace of AFM order. The measurement of nuclear spin-lattice relaxation rate $1/T_1$, that probes the development of low-lying magnetic excitations, revealed a distinct peak at T_c , followed by a $1/T_1 T = \text{const}$ behavior well below T_c .⁸

Quite recently, Takimoto and Moriya have studied an interplay between antiferromagnetism and superconductivity by using the spin-fluctuation theory within the fluctuation-exchange (FLEX) approximation.¹⁵ They have found that d -wave superconductivity coexists with an incommensurate spin-density wave (SDW) and that soft components of incommensurate SDW spin fluctuations grow as the coexistence phase is approached. Also, they have calculated the temperature (T) dependence of $1/T_1 T$ which shows a sharp peak at T_c , followed by a saturation in $1/T_1 T$ below T_c . This result is in good agreement with the experimental results in $1/T_1 T$ for Ce_{0.99}Cu_{2.02}Si₂ and hence reinforces that Ce_{0.99}Cu_{2.02}Si₂ is located at the border of the AFM phase. Remarkably, the recent μ SR experiment has demonstrated that the exotic superconductivity in Ce_{0.99}Cu_{2.02}Si₂ coexists in a microscopic level with slowly fluctuating AFM waves.¹⁶ This result has suggested that the superconductivity and the marginal AFM state in CeCu₂Si₂ have a common background.

Such an exotic coexistent phase is tuned in a delicate way

by varying a coupling constant $g = |J_{cf}|/W$, where $|J_{cf}|$ is the exchange coupling constant between the $4f$ moment and conduction-electron spin and W the bandwidth of the conduction electron. As a matter of fact, the slowly fluctuating AFM waves are depressed completely by applying pressures exceeding $P = 0.2$ GPa, i.e., the increase of g .¹⁷ The normal state is well described in terms of the self-consistent renormalized (SCR) AFM spin-fluctuation theory. The HF SC state with a line-node gap manifests itself under such an AFM Fermi liquid state.

On the other hand, the Ge substitution for Si expands the lattice, leading to the reduction of g . Therefore, it would be expected that magnetic [Ruderman-Kittel-Kasuya-Yosida (RKKY)] interactions of $4f$ moments become stronger as Ge content (x) increases. In fact, only 2% Ge substitution ($x = 0.02$) leads to an emergence of AFM order at $T_N = 0.75$ K, followed by the SC transition at $T_c = 0.4$ K.¹⁸ With increasing x , T_N is increased, but T_c is steeply decreased. Note, on the one hand, that the SC transition survives up to $x \sim 0.15$ and the superconductivity at $x = 0.1$ was suggested to be of HF origin, coexisting with AFM order.¹⁹

In the previous paper,¹⁸ superconductivity ($T_c = 0.4$ K) and antiferromagnetism ($T_N = 0.75$ K) were suggested to coexist in $\text{CeCu}_2(\text{Si}_{0.98}\text{Ge}_{0.02})_2$. It was proposed that the exotic SC phase in the nearly homogeneous sample and the coexistence of AFM and SC phases in the slightly Ge-substituted sample can be accounted for on the basis of SO(5) theory that unifies superconductivity and antiferromagnetism.^{18,20} We believe that this model could shed light on current ideas regarding the magnetically mediated mechanism of the superconductivity in other strongly correlated electron systems in addition to high- T_c cuprates.

In order to gain further insight into an interplay between superconductivity and antiferromagnetism, it is important to investigate how magnetic and SC properties change as x is increased or as g is decreased. In this study, we have carried out Cu-NQR measurements on $\text{CeCu}_2(\text{Si}_{1-x}\text{Ge}_x)_2$ in $0 < x \leq 0.2$. Note that the isostructural CeCu_2Ge_2 exhibits the AFM order below $T_N = 4.15$ K at $P = 0$,^{21,22} but it turned out

to exhibit the HF superconductivity at pressures exceeding 7.6 GPa.^{1,23} Remarkable results are presented as follows. (1) The AFM order emerges suddenly at $T_N = 0.7$ K by substituting only 1% Ge for Si, followed by the SC transition at $T_c = 0.5$ K. The sudden emergence of the AFM order reinforces that the exotic magnetic phase at $x = 0$ is in fact the marginal AFM state where the slowly fluctuating AFM waves propagate over a long distance. (2) The appearance of internal field (H_{int}) throughout the sample, that is deduced from an NQR spectral shape below T_c , excludes the presence of phase segregation between the SC and the AFM phase in the coexistent state below T_N . However, no significant anomalies in $1/T_1$ and NQR spectrum are observed below T_c , suggesting the persistence of magnetic excitations even in the coexistent phase. (3) As x increases, T_N is progressively increased, but T_c is steeply decreased. As a result of the suppression of the slowly fluctuating AFM waves in the samples with more than $x = 0.06$, their magnetic properties above T_N progressively change to those in a localized regime as observed in CeCu_2Ge_2 .

II. EXPERIMENT AND RESULT

Samples of $\text{CeCu}_2(\text{Si}_{1-x}\text{Ge}_x)_2$ at $x = 0.01, 0.02, 0.04, 0.06, 0.1,$ and 0.2 were prepared as described elsewhere.¹⁹ These samples were moderately crushed into grains with diameters larger than $100 \mu\text{m}$ in order to avoid some crystal distortion, if any. A SC transition temperature T_c was confirmed by a distinct change in inductance of NQR coil. As x increases, T_c decreases steeply as $T_c = 0.5, 0.4, 0.2,$ and 0.15 for $x = 0.01, 0.02, 0.06,$ and 0.1 , respectively. This result is totally consistent with the previous resistivity and susceptibility measurements.²⁴ The NQR spectrum was obtained by measuring a spin-echo intensity as a function of frequency, using a phase coherent pulsed NMR spectrometer. The nuclear spin-lattice relaxation rate $1/T_1$ was measured by the conventional saturation-recovery method.

Figure 1 indicates ^{63}Cu - and ^{65}Cu -NQR spectra at $x = 0.02, 0.04, 0.06, 0.1,$ and 0.2 at 4.2 K. Here, the spectrum at $x = 0.01$ is not shown, since it is nearly equivalent to that at $x = 0.02$. For $x = 0.02$, the respective main peaks at 3.435 and 3.175 MHz arise from ^{63}Cu and ^{65}Cu nuclei with nuclear spin $I = 3/2$. Satellite peaks at 3.315 and 3.064 MHz are assigned to the Cu sites around Ge atoms, since these peaks appear by substituting Ge for Si and grow up with increasing x . This kind of satellite peak is often observed, once a small amount of impurities is introduced into HF systems, for example, the La doped CeRu_2Si_2 .²⁵ As x increases, the NQR linewidth becomes broader, pointing to a large inhomogeneous distribution of the electric field gradient (EFG) at the Cu site. Nevertheless, their magnetic state is rather homogeneous through the whole sample as shown later.

A. NQR spectrum—probe of internal field due to AFM order

The previous work revealed that the slowly fluctuating AFM waves in the nearly homogeneous $\text{Ce}_{0.99}\text{Cu}_{2.02}\text{Si}_2$ ($x = 0$) evolve into the AFM order, once only 2% Ge (x

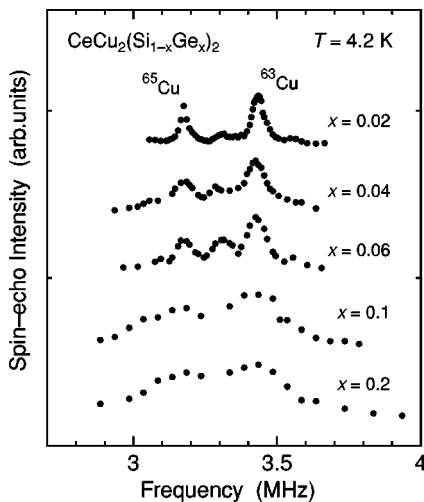


FIG. 1. $^{63,65}\text{Cu}$ -NQR spectra of $\text{CeCu}_2(\text{Si}_{1-x}\text{Ge}_x)_2$ at $x = 0.02, 0.04, 0.06, 0.1,$ and 0.2 at 4.2 K.

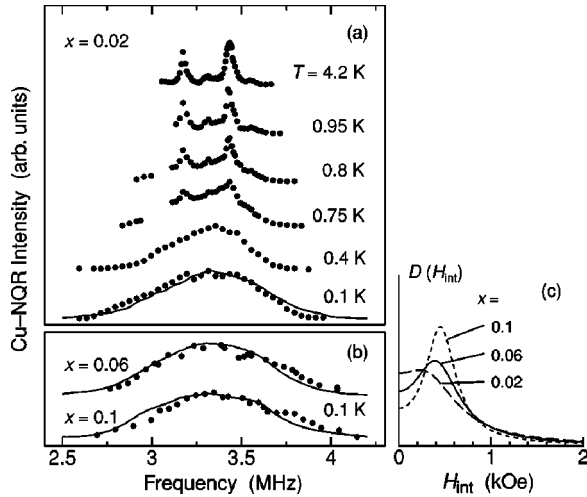


FIG. 2. (a) Temperature dependence of $^{63,65}\text{Cu}$ -NQR spectrum in $\text{CeCu}_2(\text{Si}_{0.98}\text{Ge}_{0.02})_2$ ($x=0.02$). The broadening of NQR line-width below $T_N=0.75$ K indicate the presence of internal field H_{int} at the Cu sites. (b) NQR spectra at $x=0.06$ and 0.1 at $T=0.1$ K. The solid lines are simulations where the Zeeman shift due to H_{int} is incorporated (see the text in details). (c) Distributions $D(H_{\text{int}})$ of H_{int} at the Cu sites in the ordered states at $x=0.02$, 0.06 , and 0.1 .

$=0.02$) is substituted for Si.¹⁸ This is because the NQR spectrum at $x=0.02$ undergoes a significant broadening due to the appearance of internal field H_{int} below T_N . It is noteworthy that the spectrum at $x=0$ does not show any broadening down to 0.012 K.⁸ Here, we report extensive measurement of NQR spectrum at $x=0.02$, 0.04 , 0.06 , 0.1 , and 0.2 . From a detailed analysis of it, an intimate evolution in magnetic nature is extracted.

Figure 2(a) indicates the NQR spectra at $x=0.02$ at various temperatures. It is evident that the spectral width markedly broadens below $T_N\sim 0.75$ K. The emergence of AFM order is also corroborated by the $1/T_1$ result that exhibits a sharp peak at T_N as shown in the following subsection. The T and x dependencies of NQR spectrum allow us to examine a systematic evolution of the AFM order.

A NQR spectral shape was simulated by incorporating both the distributions of EFG and H_{int} . The distribution in EFG due to the Ge substitution is obtained from the NQR spectrum in the paramagnetic state indicated in Fig. 1. The distribution in H_{int} is assumed by taking into account a possible magnetic structure reported from the neutron-diffraction results on CeCu_2Ge_2 .^{21,22}

The nuclear Hamiltonian at $H=0$ below T_N is described in terms of the nuclear electric quadrupole (eqQ) interaction and the Zeeman interaction due to H_{int} as

$$\mathcal{H}_Q = \frac{e^2qQ}{4I(2I-1)} \left[3I_z^2 - I(I+1) + \frac{\eta}{2}(I_+^2 + I_-^2) \right],$$

$$\mathcal{H}_Z = -\gamma_n \hbar I \cdot H_{\text{int}},$$

where γ_n and η are the $^{63,65}\text{Cu}$ nuclear gyromagnetic ratio and the asymmetry parameter for the EFG tensor, defined as $eq \equiv V_{ZZ}$ and $\eta \equiv (V_{XX} - V_{YY})/V_{ZZ}$, respectively. Here, $\eta \sim 0$. Note that the direction of V_{ZZ} at Cu site is parallel to

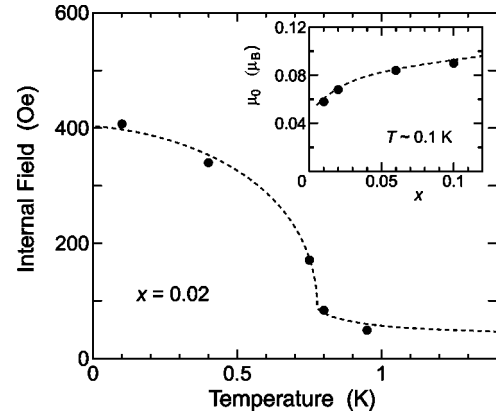


FIG. 3. Temperature dependence of $\langle H_{\text{int}} \rangle$ at $x=0.02$. The inset indicates the size of magnetic moment at 0.1 K as the function of Ge concentration. Both dotted lines are guide for eye.

the tetragonal c axis.²⁶ By resolving the total Hamiltonian $\mathcal{H} = \mathcal{H}_Q + \mathcal{H}_Z$ exactly, we calculated the eigenenergies of four nuclear-spin levels. The transition probability between the adjacent eigenstate gives an expected intensity for each resonance line. Thus, a full line shape is numerically simulated by taking both the contributions of H_{int} and ν_Q into consideration. The result at $T=0.1$ K is indicated by the solid lines at $x=0.02$ in Fig. 2(a) and $x=0.06$ and 0.1 in Fig. 2(b). The overall agreement between the experiment and the simulation seems to be satisfactory for all the results.

Thus obtained shape of distribution in H_{int} , $D(H_{\text{int}})$ is represented in Fig. 2(c). The H_{int} at a peak, $\langle H_{\text{int}} \rangle$ slightly increases as $\langle H_{\text{int}} \rangle = 0.3$, 0.4 , and 0.45 kOe at $x=0.02$, 0.06 , and 0.1 , respectively. Provided that a possible magnetic structure is of an AFM type with a wave vector $q_1 = (1/2, 1/2, c)$ in CePd_2Si_2 and CeRh_2Si_2 or with $q_2 = (0, 0, 1/2)$ in URu_2Si_2 ,²⁷⁻³² H_{int} is canceled out at the Cu sites that occupy a magnetically symmetric position. Therefore, a likely spin structure may be either helical or spin-density-wave (SDW) type. These spin structures were indicated by the elastic neutron-diffraction experiments on the $\text{CeCu}_2(\text{Si}_{1-x}\text{Ge}_x)_2$ with $x=0.6$, 0.8 , and 1 .^{21,22} The SDW type of order is, however, unlikely because $D(H_{\text{int}})$ should have a peak around $H_{\text{int}} \sim 0$ associated with the presence of nodes in SDW and a different shape from $D(H_{\text{int}})$ in Fig. 2(c) is simulated.

In contrast, in a helical spin structure, it should be noted that H_{int} is predominantly produced by four nearest-neighbor Ce moments. Therefore, $\langle H_{\text{int}} \rangle$ allows us to estimate an average ordered moment using the value of hyperfine coupling constant $A_{\parallel} = -4.6$ kOe/ μ_B in the paramagnetic state.³³ Figure 3 shows the T dependence of $\langle H_{\text{int}} \rangle$ at $x=0.02$. It seems to follow a T variation on the mean-field approximation below T_N even though coming across $T_c \sim 0.4$ K. As shown in the inset of Fig. 3, a magnetic moment $\mu_0 \sim 0.06\mu_B$ at $T=0.1$ K and $x=0.01$ increases slightly with the Ge concentration, consistent with the result from the μSR experiments.^{34,35} This AFM order with a tiny moment is consistent with the result by recent neutron-diffraction measurements.³⁶

The full width ΔH_{int} at the half maximum of $D(\langle H_{\text{int}} \rangle)$

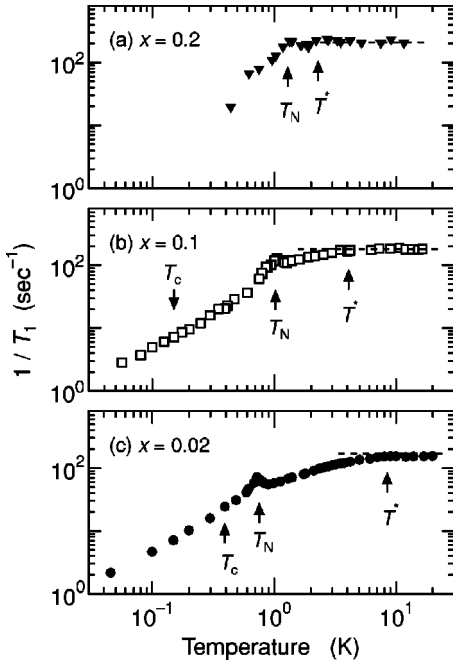


FIG. 4. Temperature dependence of the nuclear spin-lattice relaxation rate $1/T_1$ of ^{63}Cu at $x =$ (a) 0.2, (b) 0.1, and (c) 0.02.

becomes narrower as x increases. A large value of ΔH_{int} at $x=0.02$ may be explained by the combined contributions of an intrinsic distribution in H_{int} due to its helical structure and of an inevitable spatial distribution in size of spontaneous moments due to the Ge doping. In the helical structure, H_{int} consists of $H_{\text{int}}^{\parallel}$ and H_{int}^{\perp} parallel and perpendicular to the tetragonal c axis, respectively. Note that the Zeeman shift in NQR spectrum due to H_{int}^{\perp} is four times larger than that due to $H_{\text{int}}^{\parallel}$ because the principal axis of EFG is parallel to the c axis. Therefore, even when a size in H_{int} is fixed, its direction is actually distributed due to the helical structure, resulting in the large value in ΔH_{int} .

It should be mentioned that no peak in $D(H_{\text{int}})$ appears at $H_{\text{int}}=0$. The absence of peak in $D(H_{\text{int}})$ at $H_{\text{int}}=0$ excludes a possibility that the SC phase is spatially separated from the AFM phase. Because, in case of the spatial segregation between two phases, two peaks in $D(H_{\text{int}})$ at $H_{\text{int}}=0$ and $\langle H_{\text{int}} \rangle \neq 0$ might arise from SC and AFM phase, respectively. When x increases, this phase segregation due to the Ge substitution, *if any*, would induce considerable changes in the distribution in H_{int} . However, the same type of distribution in H_{int} is deduced irrespective of x . Thus, the possibility of any phase segregation is ruled out by this systematic evolution in the Cu-NQR spectra with the Ge content.

B. Nuclear spin-lattice relaxation rate $1/T_1$

The T dependence of the nuclear spin-lattice relaxation rate $1/T_1$ of ^{63}Cu at $x=0.2$, 0.1, and 0.02 is shown in Figs. 4(a), 4(b), and 4(c), respectively. $1/T_1$ is uniquely determined above T_N , but it is distributed below T_N for all the samples. The distribution in $1/T_1$ below T_N is presumably associated with the distribution of H_{int} , related to the helical magnetic structure in the AFM state. The value of faster component in

$1/T_1$ is about three times larger than that of slower one below T_N , as shown later. Only slow component in $1/T_1$ is shown below T_N for a simplicity of discussion.

In a high T region, $1/T_1$ becomes almost T independent above a temperature marked as T^* in Fig. 4, exhibiting that local-moment fluctuations dominate the relaxation process. It is known in HF systems that T^* is scaled to the quasielastic linewidth in neutron-scattering spectrum, leading to a tentative estimation of the bandwidth of HF state [$T^* \propto \exp(-1/g)$]. Therefore, the decrease in T^* due to the Ge substitution indicates the reduction of HF bandwidth. In such a localized regime above T^* , the constant value of $1/T_1$ is proportional to $p_{\text{eff}}^2 W/J_{cf}^2$, where p_{eff} is an effective paramagnetic local moment. Therefore, the progressive increase in $1/T_1$ with increasing x is ascribed to the increase in p_{eff} and/or the reduction of $|J_{cf}|$. This result is consistent with the decrease in T^* due to the reduction of $g = |J_{cf}|/W$ caused by the Ge substitution.

Next, we focus on the magnetic properties at $x=0.02$ and subsequently its evolution with increasing x . For $x=0.02$, $1/T_1$ gradually decreases down to T_N below T^* , revealing a crossover from a localized to an itinerant regime. A clear peak at $T_N=0.75$ K, below which the NQR linewidth broadens rapidly, reflects a critical slowing down associated with the AFM transition. A rapid drop of $1/T_1$ below T_N is presumably due to a partial loss of low-lying excitations.

The $1/T_1$ result nearby the AFM phase is well explained by the SCR theory for nearly or weakly AFM itinerant magnets.^{37,38} In this scheme, $1/T_1$ is predicted as follows:

$$1/T_1 \propto T \sqrt{\chi_Q(T)} \propto T / \sqrt{T - T_N}$$

above T_N ,

$$1/T_1 \propto T / M_Q(T) \propto T / \sqrt{T_N - T}$$

below T_N . Here, $\chi_Q(T)$ and $M_Q(T)$ are a dynamical susceptibility and the magnetization of AFM sublattice, respectively. The $1/T_1 T$ data at $x=0.02$ are fitted by including the term $6.6/\sqrt{T-T_N}$ in $1.5 \text{ K} > T > T_N = 0.75 \text{ K}$ and $12/\sqrt{T_N-T}$ in $T_c < T < T_N$ as presented in the inset of Fig. 5. The good agreement between the experiment and the calculation indicates a long-range nature of the AFM ordering in the itinerant regime.

By substituting Ge for Si, as indicated by arrows in Fig. 4, while T^* is decreased, T_N is gradually increased in collaboration with the development of saturation moment μ_0 . As a result, T^* approaches to T_N , indicating that the magnetic properties just above T_N change from the itinerant to localized regime. Correspondingly, the peak in $1/T_1$ at T_N disappears at $x=0.2$, resembling the behavior observed for f -electron antiferromagnets that are in the localized regime.³⁹ The SCR theory is not applicable to the data for $x=0.06$ and 0.1 any more, since the itinerant regime is limited in a narrow T range for $1/T_1$ to be fitted.

We now turn to the SC state in which low-energy properties are intimately changed by substituting Ge for Si or ap-

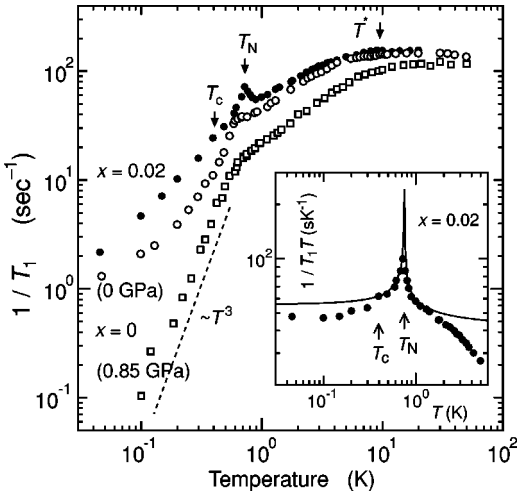


FIG. 5. Temperature dependence of $1/T_1$ for $x=0.02$ and $\text{Ce}_{0.99}\text{Cu}_{2.02}\text{Si}_2$ ($x=0$) at ambient pressure and at 0.85 GPa. The inset shows the $1/T_1 T$ vs T plot for $x=0.02$. The solid line is a fit on the basis of the SCR theory that is consistent with the data for $T_N < T < 1.5$ K and $T_c < T < T_N$ (see text).

plying P . In order to demonstrate this, the T dependence of $1/T_1$ at $x=0.02$ is indicated in Fig. 5 with those for $\text{Ce}_{0.99}\text{Cu}_{2.02}\text{Si}_2$ ($x=0$) at $P=0$ and 0.85 GPa.¹⁷ As seen in Fig. 5, the line-node SC gap at $P=0.85$ GPa is evidenced from a $1/T_1 \propto T^3$ dependence. However, the $1/T_1$ at $x=0$ is deviated well below T_c from the T^3 one and exhibits a weak T dependence. Likewise, the $1/T_1$ at $x=0.02$ is nearly proportional to the temperature far below T_N . This suggests that the low-energy spectral weight in spin-fluctuation spectrum survives even below T_c at $x=0$ and 0.02.

Here, we should remark whether or not the disorder effect associated with the Ge substitution influences the magnetic property because the satellite peak is actually observed in NQR spectrum (see Fig. 1). In order to investigate some local inhomogeneous effect, the $1/T_1$'s at $x=0.02$ were measured at the main (3.435 MHz) and the satellite (3.315 MHz) peaks. Note that the latter arises from the ^{63}Cu sites around the Ge atoms. As shown in Fig. 6, in the paramagnetic state, the value of $1/T_1$ at the satellite peak is slightly larger than that at the main peak over a whole T range. The small difference in the values of $1/T_1$ may be due to a possible difference in g . Nevertheless, both the $1/T_1$'s exhibit a distinct peak at T_N , evidencing a long-range character of AFM order. Below T_N , although both T_1 's are not uniquely determined owing to the distribution in H_{int} , the short and long components undergo a similar T dependence. Thereby the AFM order takes place throughout the whole sample, although it is not completely excluded that the size in spontaneous moments is spatially distributed.

One may suspect that the potential scattering due to non-magnetic Ge impurities brings about a finite density of states at the Fermi surface, leading to the observed enhancement of $1/T_1$ below T_c .^{41,42} However, a recent NQR result under P at $x=0.02$ reveals that the AFM order is suppressed and the HF superconductivity with the line-node gap is recovered

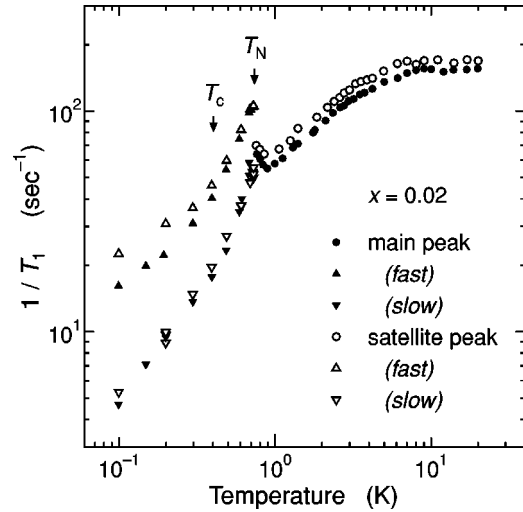


FIG. 6. Temperature dependence of $1/T_1$ at $x=0.02$, measured at a main peak of 3.435 MHz (closed symbols) and a satellite peak of 3.315 MHz (open symbols). The fast and slow relaxation components owing to the distribution in internal field are estimated for each below T_N .

by applying pressures.⁴⁰ This result apparently excludes such the impurity effect as a cause for the enhancement of $1/T_1$ below T_c .

C. Temperature dependence of NQR intensity probing the marginal AFM state

Figures 7(a) and (b) indicate the T dependence of NQR intensity multiplied by temperature [$I(T) \times T$] at $x=0.06$ and 0.02 along with that [Fig. 7(c)] at $x=0$ reported previously.⁸ Here, $I(T)$ is an integrated intensity over the NQR spectrum and normalized by the value at 4.2 K. Since an NQR intensity depends on a pulse interval τ between two

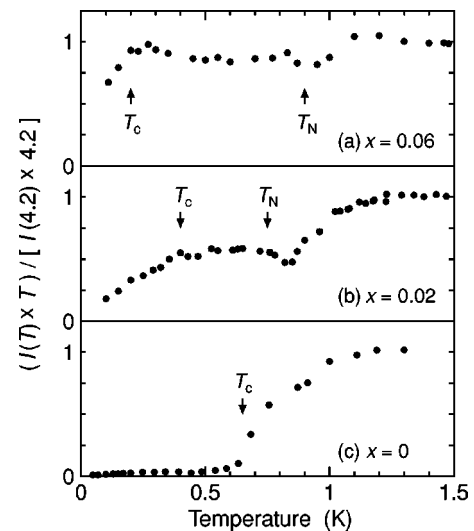


FIG. 7. Temperature dependence of $I(T) \times T$ where $I(T)$ is an NQR intensity normalized by the value at 4.2 K at (a) $x=0.06$, (b) 0.02 in $\text{CeCu}(\text{Si}_{1-x}\text{Ge}_x)_2$, and (c) the undoped $\text{Ce}_{0.99}\text{Cu}_{2.02}\text{Si}_2$ ($x=0$).

pulses by means of the spin-echo method, $I(\tau=0)$ is evaluated through the relation of $I(\tau)=I(\tau=0)\exp(-2\tau/T_2)$ where, $1/T_2$ is the spin-echo decay rate. $I(T)$ is generally proportional to $1/T$ following to the Curie susceptibility for a nuclear-spin system. Therefore, $I(T)\times T$ should stay constantly if the nuclear relaxation time ranges in an observable time window that is typically more than several microseconds. Therefore, the large reduction of $I(T)\times T$ on cooling at $x=0$ is ascribed to the development of the slowly fluctuating AFM waves. Note that a $T_1\sim 0.14\ \mu\text{sec}$, that is estimated from the relation $1/T_1\propto\omega_c(T)/[\omega_c(T)^2+\omega_{\text{NQR}}^2]$, is too short for the NQR signal to be observed experimentally. Here, ω_c ($\sim 3\ \text{MHz}$) and ω_{NQR} ($\sim 3.4\ \text{MHz}$) is a characteristic frequency of the slowly fluctuating AFM waves and the central NQR frequency, respectively.⁹

We now turn to the result on the Ge substituted compounds. The $I(T)\times T$ at $x=0.02$ decreases down to ~ 0.4 upon cooling from 1.2 K down to $T_N=0.75\ \text{K}$, resembling the behavior at $x=0$. The reduction of $I(T)\times T$ stops around T_N , but does not recover with further decreasing T . Note that the reduction below $T_c=0.4\ \text{K}$ is due to the SC diamagnetic shielding of rf field for the NQR measurement. Apparently, the AFM order, that suddenly appears at $x=0.02$, coexists with the marginal AFM state. It seems, therefore, that the onset of AFM order due to the lattice expansion is indicative of a first-order type.

By contrast, the $I(T)\times T$ at $x=0.06$ does not decrease significantly upon cooling down to $T_c=0.2\ \text{K}$ across $T_N=0.9\ \text{K}$. It indicates that the slowly fluctuating AFM waves are not appreciable above $x=0.06$ and that the magnetic property changes to a rather conventional type of behavior with increasing x . The μSR measurements also suggest a change toward more static character of the magnetic phase with increasing x .³⁵

III. DISCUSSION

Figure 8 shows the phase diagram determined against the Ge content (x) on $\text{CeCu}_2(\text{Si}_{1-x}\text{Ge}_x)_2$ and the pressure on $\text{Ce}_{0.99}\text{Cu}_{2.02}\text{Si}_2$ ($x=0$). Here we expect that a primary effect of the Ge doping is to expand the lattice and that its chemical pressure is $-7.6\ \text{GPa}$ per 100% Ge doping as suggested from the P dependence of ν_Q in CeCu_2Ge_2 and CeCu_2Si_2 .⁴³ The data at $x=0$ under P are cited from the previous paper.¹⁷ The characteristic temperature T^* which is scaled to the bandwidth of HF band, increases continuously with the lattice compression by decreasing x and increasing P . T_N is determined as the temperature below which H_{int} develops and at which $1/T_1$ exhibits a peak. T_c is obtained from this work. The slowly fluctuating AFM waves develop below T_m in $0\leq x<0.06$ and $0<P<0.2\ \text{GPa}$. Remarkably the marginal AFM state emerges only close to the border between AFM and SC phases.

The AFM order suddenly sets in once slight Ge is substituted for Si. By contrast, any trace of AFM order is not observed down to 0.012 K at $x=0$. With increasing x , T_N is progressively increased, while T_c is steeply decreased. Correspondingly, the slowly fluctuating AFM waves are suppressed for the samples with more than $x=0.06$. It is note-

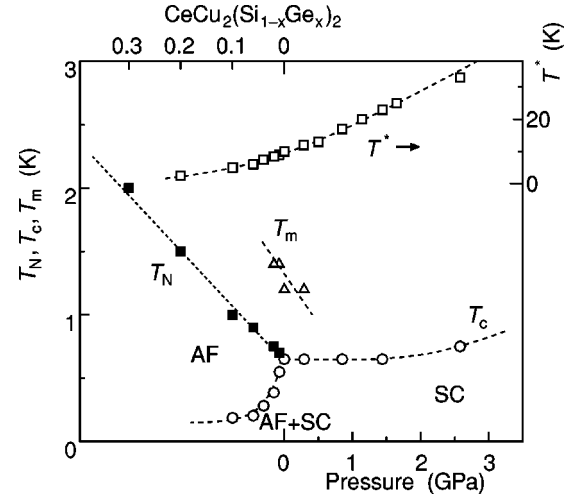


FIG. 8. The AFM and SC combined phase diagram for $\text{CeCu}_2(\text{Si}_{1-x}\text{Ge}_x)_2$ and for $\text{Ce}_{0.99}\text{Cu}_{2.02}\text{Si}_2$ ($x=0$) under pressure. T_N (closed squares) and T_c (open circles) are the AFM and SC transition temperature, respectively. Also shown are the characteristic temperature to be scaled to the band width of HF state T^* (open squares) and T_m below which the marginal AFM state develops (open triangles). The data for $x=0$ under pressure are cited from a previous paper (Ref. 17).

worthy that the AFM order seems to suddenly disappear at $x=0$ as if T_N was replaced by T_c . Eventually, the superconductivity coexists with the marginal AFM state at $x=0$. This fact suggests that antiferromagnetism and superconductivity have a common background.

In $0<P<0.2\ \text{GPa}$, the marginal AFM state is expelled by the onset of superconductivity below T_c at $H=0$. However, when H turns on to suppress the superconductivity, the first-order like transition from SC state to the magnetic phase A takes place.⁵ In $P>0.2\ \text{GPa}$, the marginal AFM state is completely suppressed and, at the same time, the typical HF superconductivity is recovered with the line-node SC gap.

Next, we shed further light on the coexisting state by comparing with the typical HF superconductor UPd_2Al_3 where the AFM order sets in below $T_N\sim 14.5\ \text{K}$, followed by the onset of typical SC transition below $T_c\sim 1.98\ \text{K}$.⁴⁴⁻⁴⁶ In UPd_2Al_3 , the coexistence of the AFM order with the superconductivity has been established by various measurements.^{45,47-49} The Al- and Pd-NQR results showed that $1/T_1$ decreases rapidly because a gap opens at a part of the Fermi surface below T_N and follows the $1/T_1\propto T^3$ below T_c , consistent with the line-node SC gap.^{47,48} In UPd_2Al_3 , note that an average occupation of $5f$ electrons per U atom is slightly less than three and larger than one in Ce-based HF systems.⁵⁰ With some relevance with this, nearly two localized $5f$ electrons are responsible for the AFM order, carrying the relatively large spontaneous moment of $0.85\mu_B$ per U atom. Since the spin-wave excitations in the AFM state are gapped, the particle-hole excitations in HF state are dominant well below T_N , as actually evidenced from the $T_1T=\text{const}$ behavior typical for the Fermi liquid state. Therefore, the $1/T_1$ in the SC state is not affected by the magnetic excitations even in the coexistent state, but reflects its line-

node SC gap structure. However, the situation in underlying CeCu_2Si_2 is completely different, because one $4f$ electron per Ce ion plays vital roles for both the magnetism and the superconductivity, leading to the novel interplay between the magnetism and the superconductivity revealed in CeCu_2Si_2 .

Apparently, the exotic AFM and SC phases in $0 \leq x < 0.06$ may be new states of matter. In a previous paper,¹⁸ we proposed that the coexistence of AFM and SC phases in the slightly Ge substituted compounds and the magnetic-field induced phase A in $0 < P < 0.2$ GPa are accounted for on the basis of the SO(5) theory.^{18,20} It is considered that the marginal AFM state in $0 \leq x < 0.06$ below T_c may be identified as a collective magnetic mode in the coexisting phase and that it turns out to be competitive with the onset of SC phase in $0 < P < 0.2$ GPa at $H=0$. The latter is relevant to the emergence of the field-induced first-order-like SC to magnetic phase A transition. Concerning the interplay between magnetism and superconductivity, we would propose that the marginal AFM state in the SC state at $x=0$ may correspond to a pseudo-Goldstone mode due to the broken U(1) symmetry. Due to the closeness to a magnetic critical point, however, such a gapped mode in the SC state should be characterized by an extremely tiny excitation (resonance) energy. We thus believe that this SO(5) model could shed light on the intimate interplay between magnetism and superconductivity in CeCu_2Si_2 that has been an issue for over a decade.

Finally, we compare the present experimental results with those on $\text{Ce}_{0.975}\text{Cu}_2\text{Si}_2$ ($\text{Ce}_{0.975}$) where an AFM order was reported below $T_N \sim 0.6$ K.^{8,13} Unlike the Ge substituted samples, any signature of superconductivity was not observed and the AFM order persists up to $P=2$ GPa in $\text{Ce}_{0.975}$.⁵¹ The recent NQR result under P at $x=0.02$ has revealed that the AFM order is suppressed and the HF superconductivity with the line-node gap is recovered at small pressure.⁴⁰ These results indicate that the AFM order in $\text{Ce}_{0.975}$ is driven by some disorder effect that destroys the superconductivity. By contrast, the AFM order at $x=0.02$ is

due to the lattice expansion by the Ge substitution for Si. Therefore, the induced AFM order may be able to coexist with the superconductivity without destroying it.

IV. CONCLUSION

We have investigated magnetic and superconducting properties in $\text{CeCu}_2(\text{Si}_{1-x}\text{Ge}_x)_2$ with $0 < x \leq 0.2$ by means of the Cu-NQR measurement. The Ge substitution for Si acts as a chemical negative pressure. Once 1% Ge is substituted for Si to expand the lattice of $x=0$, the AFM order sets in at $T_N \sim 0.7$ K, followed by the onset of superconductivity below $T_c=0.5$ K. The AFM order is evidenced by both the broadening of the Cu-NQR spectrum and the distinct peak in $1/T_1$ at T_N . This sudden emergence of AFM order due to the slight Ge substitution reinforces that the exotic magnetic phase in the undoped $\text{Ce}_{0.99}\text{Cu}_{2.02}\text{Si}_2$ ($x=0$) is in fact the marginal AFM state where the slowly fluctuating AFM waves propagate over a long distance. With increasing x , T_N is progressively increased, while T_c is rather steeply decreased. The appearance of the internal field throughout the sample, that was deduced from the NQR spectrum below T_N , excludes the presence of phase segregation between the SC and the AFM phases in the coexistent state. The $1/T_1$ result does not show any significant reduction below T_c , followed by the $T_1 T = \text{const}$ behavior. It suggests that the SC phase is in the gapless regime dominated by the magnetic excitations presumably due to the coexistence of AFM and SC phases.

ACKNOWLEDGMENTS

We thank A. Koda, W. Higemoto, and R. Kadono for valuable discussions. This work was supported by the COE Research in Grant-in-Aid for Scientific Research from the Ministry of Education, Culture, Sports, Science and Technology of Japan (Grant No. 10CE2004). One of the authors (Y.K.) was supported by the JSPS.

*Present address: Department of Physics, Faculty of Engineering, Tokushima University, Tokushima 770-8506, Japan

†Present address: Department of Physics, Graduate School of Science, Kyoto University, Kyoto 606-8502, Japan

¹D. Jaccard, K. Behnia, and J. Sierro, *Phys. Lett. A* **163**, 475 (1992).

²R. Movshovich, T. Graf, D. Mandrus, J. D. Thompson, J. L. Smith, and Z. Fisk, *Phys. Rev. B* **53**, 8241 (1996).

³N. D. Mathur, F. M. Grosche, S. R. Julian, I. R. Walker, D. M. Freye, R. K. W. Haselwimmer, and G. G. Lonzarich, *Nature (London)* **394**, 39 (1998).

⁴H. Hegger, C. Petrovic, E. G. Moshopoulou, M. F. Hundley, J. L. Sarrao, Z. Fisk, and J. D. Thompson, *Phys. Rev. Lett.* **84**, 4986 (2000).

⁵G. Bruls, B. Wolf, D. Finsterbusch, P. Thalmeier, I. Kouroudis, W. Sun, W. Assmus, B. Lüthi, M. Lang, K. Gloos, F. Steglich, and R. Modler, *Phys. Rev. Lett.* **72**, 1754 (1994).

⁶H. Nakamura, Y. Kitaoka, H. Yamada, and K. Asayama, *J. Magn. Mater.* **76&77**, 517 (1988).

⁷Y. J. Uemura, W. J. Kossler, X. H. Yu, H. E. Schone, J. R. Kemp-

ton, C. E. Stronach, S. Barth, F. N. Gyax, B. Hitti, A. Schenck, C. Baines, W. F. Lankford, Y. Onuki, and T. Komatsubara, *Phys. Rev. B* **39**, 4726 (1989).

⁸K. Ishida, Y. Kawasaki, K. Tabuchi, K. Kashima, Y. Kitaoka, K. Asayama, C. Geibel, and F. Steglich, *Phys. Rev. Lett.* **82**, 5353 (1999).

⁹R. Feyerherm, A. Amato, C. Geibel, F. N. Gyax, P. Hellmann, R. H. Heffner, D. E. MacLaughlin, R. Müller-Reisener, G. J. Nieuwenhuys, A. Schenk, and F. Steglich, *Physica B* **206-207**, 596 (1995); *Phys. Rev. B* **56**, 699 (1997).

¹⁰A. W. Hunt, P. M. Singer, K. R. Thurber, and T. Imai, *Phys. Rev. Lett.* **82**, 4300 (1999).

¹¹N. J. Curro, P. C. Hammel, B. J. Suh, M. Hücker, B. Büchner U. Ammerahl, and A. Revcolevschi, *Phys. Rev. Lett.* **85**, 642 (2000).

¹²F. Steglich, B. Buschinger, P. Gegenwart, M. Lohmann, R. Hellfrich, C. Langhammer, P. Hellmann, L. Donnevert, S. Thomas, A. Link, C. Geibel, M. Lang, G. Sparn, and W. Assmus, *J. Phys.: Condens. Matter* **8**, 9909 (1996).

¹³R. Modler, M. Lang, C. Geibel, C. Schank, R. Müller-Reisener, P.

- Hellmann, A. Link, G. Sparn, W. Assmus, and F. Steglich, *Physica B* **206-207**, 586 (1995).
- ¹⁴P. Gegenwart, C. Langhammer, C. Geibel, R. Helfrich, M. Lang, G. Sparn, F. Steglich, R. Horn, L. Donnevert, A. Link, and W. Assmus, *Phys. Rev. Lett.* **81**, 1501 (1998).
- ¹⁵T. Takimoto and T. Moriya, *Phys. Rev. B* **66**, 134516 (2002).
- ¹⁶A. Koda, W. Higemoto, R. Kadono, Y. Kawasaki, K. Ishida, Y. Kitaoka, C. Geibel, and F. Steglich, *J. Phys. Soc. Jpn.* **71**, 1327 (2002).
- ¹⁷Y. Kawasaki, K. Ishida, T. Mito, C. Thessieu, G.-q. Zheng, Y. Kitaoka, C. Geibel, and F. Steglich, *Phys. Rev. B* **63**, 140501(R) (2001).
- ¹⁸Y. Kitaoka, K. Ishida, Y. Kawasaki, O. Trovarelli, C. Geibel, and F. Steglich, *J. Phys.: Condens. Matter* **13**, L79 (2001).
- ¹⁹O. Trovarelli, M. Weiden, R. Müller-Reisener, M. Gómez-Berisso, P. Gegenwart, M. Deppe, C. Geibel, J. G. Sereni, and F. Steglich, *Phys. Rev. B* **56**, 678 (1997).
- ²⁰S. C. Zhang, *Science* **275**, 1089 (1997).
- ²¹G. Knebel, C. Eggert, D. Engelmann, R. Viana, A. Krimmel, M. Dressel, and A. Loidl, *Phys. Rev. B* **53**, 11 586 (1996).
- ²²G. Knopp, A. Loidl, K. Knorr, L. Pawlak, M. Duczmal, R. Caspary, U. Gottwick, H. Spille, F. Steglich, and A. P. Murani, *Z. Phys. B: Condens. Matter* **77**, 95 (1989).
- ²³T. C. Kobayashi, T. Miyazu, N. Takeshita, K. Shimizu, K. Amaya, Y. Kitaoka, and Y. Ōnuki, *J. Phys. Soc. Jpn.* **67**, 996 (1998).
- ²⁴P. Gegenwart (unpublished).
- ²⁵H. Okura, K. Ishida, Y. Kawasaki, Y. Kitaoka, Y. Yamamoto, Y. Miyako, T. Fukuhara, and K. Maezawa, *Physica B* **281-282**, 61 (2000).
- ²⁶T. Ohama, H. Yasuoka, D. Mandrus, Z. Fisk, and J. L. Smith, *J. Phys. Soc. Jpn.* **64**, 2628 (1995).
- ²⁷B. H. Grier, J. M. Lawrence, V. Murgai, and R. D. Parks, *Phys. Rev. B* **29**, 2664 (1984).
- ²⁸R. A. Steeman, E. Frikkee, R. B. Helmholtz, A. A. Menovsky, J. van den Berg, G. J. Nieuwenhuys, and J. A. Mydosh, *Solid State Commun.* **66**, 103 (1988).
- ²⁹T. Graf, M. F. Hundley, R. Modler, R. Movshovich, J. D. Thompson, D. Mandrus, R. A. Fisher, and N. E. Phillips, *Phys. Rev. B* **57**, 7442 (1998).
- ³⁰S. Kawarazaki, M. Sato, Y. Miyako, N. Chigusa, K. Watanabe, N. Metoki, Y. Koike, and M. Nishi, *Phys. Rev. B* **61**, 4167 (2000).
- ³¹Y. Kawasaki, K. Ishida, Y. Kitaoka, and K. Asayama, *Phys. Rev. B* **58**, 8634 (1998).
- ³²C. Broholm, J. K. Kjems, W. J. L. Buyers, P. Matthews, T. T. M. Palstra, A. A. Menovsky, and J. A. Mydosh, *Phys. Rev. Lett.* **58**, 1467 (1987); C. Broholm, H. Lin, P. Matthews, T. E. Mason, W. J. L. Buyers, M. F. Collins, A. A. Menovsky, J. A. Mydosh, and J. K. Kjems, *Phys. Rev. B* **43**, 12 809 (1991).
- ³³K. Ueda, Y. Kitaoka, H. Yamada, Y. Kohori, T. Kohara, and K. Asayama, *J. Phys. Soc. Jpn.* **56**, 867 (1987).
- ³⁴W. Higemoto (unpublished).
- ³⁵A. Amato (unpublished).
- ³⁶O. Stockert (private communication).
- ³⁷T. Moriya and T. Takimoto, *J. Phys. Soc. Jpn.* **60**, 2122 (1992).
- ³⁸S. Nakamura, T. Moriya, and K. Ueda, *J. Phys. Soc. Jpn.* **65**, 4026 (1996).
- ³⁹C. Thessieu, K. Ishida, S. Kawasaki, T. Mito, Y. Kawasaki, G.-q. Zheng, Y. Kitaoka, and Y. Ōnuki, *Physica B* **281-282**, 9 (2000).
- ⁴⁰Y. Kawasaki, K. Ishida, K. Obinata, T. Mito, G.-q. Zheng, Y. Kitaoka, C. Geibel, and F. Steglich, *Physica B* **312-313**, 428 (2002).
- ⁴¹S. Schmitt-Rink, K. Miyake, and C. M. Varma, *Phys. Rev. Lett.* **57**, 2575 (1986).
- ⁴²K. Ishida, Y. Kitaoka, N. Ogata, T. Kamino, K. Asayama, J. R. Cooper, and N. Athanassopoulos, *J. Phys. Soc. Jpn.* **62**, 2803 (1993).
- ⁴³Y. Kitaoka, H. Tou, G.-q. Zheng, K. Ishida, K. Asayama, T. C. Kobayashi, A. Kohda, N. Takashita, K. Amaya, C. Geibel, C. Schank, and F. Steglich, *Physica B* **206-207**, 55 (1995).
- ⁴⁴C. Geibel, C. Shank, S. Thies, H. Kitazawa, C. D. Bredl, A. Bohm, M. Rau, A. Grauel, R. Caspary, R. Helfrich, U. Ahlheim, G. Weber, and F. Steglich, *Z. Phys. B: Condens. Matter* **84**, 1 (1991).
- ⁴⁵N. Sato, N. Aso, G. H. Lander, B. Roessli, T. Komatsubaru, and Y. Endoh, *J. Phys. Soc. Jpn.* **66**, 2981 (1997).
- ⁴⁶N. Metoki, Y. Haga, Y. Koike, N. Aso, and Y. Ōnuki, *J. Phys. Soc. Jpn.* **66**, 2560 (1997).
- ⁴⁷H. Tou, Y. Kitaoka, K. Asayama, C. Geibel, C. Schank, and F. Steglich, *J. Phys. Soc. Jpn.* **64**, 725 (1995).
- ⁴⁸K. Matsuda, Y. Kohori, and T. Kohara, *Phys. Rev. B* **55**, 15 223 (1997).
- ⁴⁹R. Caspary, P. Hellmann, M. Keller, G. Sparn, C. Wassilew, R. Kohler, C. Geibel, C. Schank, F. Steglich, and N. E. Phillips, *Phys. Rev. Lett.* **71**, 2146 (1993).
- ⁵⁰S. Yotsuhashi, H. Kusunose, and K. Miyake, *J. Phys. Soc. Jpn.* **70**, 186 (2001).
- ⁵¹Y. Kawasaki, K. Ishida, Y. Kitaoka, K. Asayama, Y. Geibel, and F. Steglich, *Physica B* **282**, 14 (2000).